Enzymatic activity of Lecithin:retinol acyltransferase: A thermostable and highly active enzyme with a likely mode of interfacial activation

ARTICLE *in* BIOCHIMICA ET BIOPHYSICA ACTA (BBA) - PROTEINS & PROTEOMICS · JUNE 2014

Impact Factor: 2.75 · DOI: 10.1016/j.bbapap.2014.02.022

7 AUTHORS, INCLUDING:

Habib Horchani
Laval University
29 PUBLICATIONS **245** CITATIONS
SEE PROFILE

Sylvain Bussières
CHU de Québec
9 PUBLICATIONS **88** CITATIONS
SEE PROFILE

Biochimica et Biophysica Acta 1844 (2014) 1128–1136

Contents lists available at ScienceDirect

Biochimica et Biophysica Acta

journal homepage: www.elsevier.com/locate/bbapap

Enzymatic activity of Lecithin:retinol acyltransferase: A thermostable and highly active enzyme with a likely mode of interfacial activation

Habib Horchani [1], Sylvain Bussières [1], Line Cantin, Mustapha Lhor, Jean-Sébastien Laliberté-Gemme, Rock Breton, Christian Salesse *

CUO-Recherche, Hôpital du Saint-Sacrement, Centre de Recherche du CHU de Québec, Québec, Québec, Canada
Département d'Ophtalmologie, Faculté de Médecine, Université Laval, Québec, Québec, Canada
Regroupement Stratégique PROTEO, Université Laval, Québec, Québec, Canada

ARTICLE INFO

Article history:
Received 29 January 2014
Received in revised form 21 February 2014
Accepted 25 February 2014
Available online 5 March 2014

Keywords:
Lecithin:retinol acyltransferase
Truncated LRAT
Visual cycle
Enzymatic activity
Retinol
Thermostability

ABSTRACT

Lecithin:retinol acyltransferase (LRAT) plays a major role in the vertebrate visual cycle. Indeed, it is responsible for the esterification of all-trans retinol into all-trans retinyl esters, which can then be stored in microsomes or further metabolized to produce the chromophore of rhodopsin. In the present study, a detailed characterization of the enzymatic properties of truncated LRAT (tLRAT) has been achieved using *in vitro* assay conditions. A much larger tLRAT activity has been obtained compared to previous reports and to an enzyme with a similar activity. In addition, tLRAT is able to hydrolyze phospholipids bearing different chain lengths with a preference for micellar aggregated substrates. It therefore presents an *interfacial activation* property, which is typical of classical phospholipases. Furthermore, given that stability is a very important quality of an enzyme, the influence of different parameters on the activity and stability of tLRAT has thus been studied in detail. For example, storage buffer has a strong effect on tLRAT activity and high enzyme stability has been observed at room temperature. The thermostability of tLRAT has also been investigated using circular dichroism and infrared spectroscopy. A decrease in the activity of tLRAT was observed beyond 70 °C, accompanied by a modification of its secondary structure, i.e. a decrease of its α-helical content and the appearance of unordered structures and aggregated β-sheets. Nevertheless, residual activity could still be observed after heating tLRAT up to 100 °C. The results of this study highly improved our understanding of this enzyme.

1. Introduction

Lecithin:retinol acyltransferase (LRAT; EC 2.3.1.135) is a very important enzyme of the visual cycle. It catalyzes the esterification of retinol into retinyl esters in the retinal pigment epithelium (RPE) as well as in other tissues including testis, liver, and intestine [1–4]. The amino acid sequence of LRAT does not show any homology to enzymes that catalyze similar reactions, such as lecithin cholesterol acyltransferase (LCAT) [5,6], and is not related either to any protein of known function. LRAT was thus described as the founder member of a new class of Cys-His enzymes of unknown function [7–9] which includes class II tumor suppressors and a group of putative viral proteases [10–13]. The enzymatic reaction catalyzed by LRAT occurs in three steps: 1) it shows a phospholipase A1 activity leading to the hydrolysis of the *sn*-1 fatty acyl chain of phospholipids; 2) this fatty acyl chain is then used to self-acylate its Cys161; 3) this acyl group is finally transferred to all-*trans* retinol through an esterification reaction [1,2,4,14,15]. The formation of a thioester intermediate resulting from the addition of an acyl chain on Cys161 has clearly been demonstrated by mass spectrometry after incubation of tLRAT with phosphatidylcholine substrates [14]. This esterified form of retinol can thereby be accumulated in microsomes for storage, or hydrolyzed and isomerized by RPE65 to form 11-*cis*-retinol [16,17] which is then further metabolized to produce the chromophore of rhodopsin (for a review, see [7,18–22]).

The primary sequence of LRAT is made of 230 amino acids with a calculated mass of 25.3 kDa [8]. This sequence suggests the existence of N- and C-terminal hydrophobic segments at positions 9–31 and 195–222, respectively [8]. Only the C-terminal transmembrane domain has been suggested to be essential for membrane targeting [23]. However, these two individual hydrophobic segments were shown to bear the same

Abbreviations: BSA, bovine serum albumin; cmc, critical micellar concentration; DHPC, 1,2-diheptanoyl-*sn*-glycero-3-phosphocholine; DMF, dimethylformamide; DPPC, 1,2-dipalmitoyl-*sn*-glycero-3-phosphocholine; DTT, dithiothreitol; LRAT, lecithin:retinol acyltransferase; tLRAT, truncated form of LRAT; MES, 2-(*N*-morpholino)ethanesulfonic acid; OG, octyl β-D-glucopyranoside; RPE, retinal pigment epithelium; SDS, sodium dodecyl sulfate

* Corresponding author at: CUO-Recherche, Centre de recherche du CHU de Québec, Hôpital du Saint-Sacrement, 1050 Chemin Ste-Foy, Québec, Québec G1S 4L8, Canada. Tel.: +1 418 682 7569; fax: +1 418 682 8000.
E-mail address: christian.salesse@fmed.ulaval.ca (C. Salesse).

[1] These authors have contributed equally to this work. They should thus be considered as co-first authors.

http://dx.doi.org/10.1016/j.bbapap.2014.02.022
1570-9639/

α-helical secondary structure and orientation in model membranes [24]. In every instance, full-length LRAT could not yet be overexpressed in *E. coli* [25] and expression in HEK (human embryonic kidney) cells has only led to a partially purified form of the protein [8], probably due to the very hydrophobic behavior of the enzyme termini [26]. A recombinant truncated form of LRAT (tLRAT) (amino acids 31–196), whose N- and C-terminal hydrophobic segments have been removed, has been produced [25]. The three essential residues forming the catalytic triad of LRAT (H60, C161 and Y154) are located within the sequence of this truncated enzyme [27]. tLRAT could thus be used to characterize the enzymatic properties of this enzyme. However, a detergent is required to achieve water-solubility of tLRAT [25] and enzymatic assays resulted in the measurement of a very low activity of this enzyme [9,25,27] compared to another enzyme having a similar activity (LCAT) [28]. Consequently, the enzymatic and biochemical properties of tLRAT must be thoroughly characterized using more appropriate experimental conditions. Moreover, thermal and time-dependent stability of tLRAT must be assayed because activity and stability are the most important qualities of enzymes [29,30], and also since the more general relationship between these properties and protein structure is still not well understood [29,30].

The present study was thus undertaken to perform a detailed characterization of the enzymatic and biochemical properties as well as of the thermal and time-dependent stability of tLRAT using in vitro assay conditions. The enzymatic properties of tLRAT and the effect of different parameters on its activity have been studied in detail, such as the usefulness of different detergents, the levels of the substrates, the pH and temperature of the enzymatic assay, the chain length selectivity of the phospholipid substrate, the content of BSA in the reaction mixture as well as the importance of the storage buffer and storage temperature and the influence of time on the activity of this enzyme. Furthermore, the thermal stability of tLRAT enzyme activity has been characterized and its related structural modifications were determined using circular dichroism and infrared spectroscopy.

2. Experimental procedures

2.1. Materials

The expression vector pET11a and the *E. coli* BL21(DE3) pLysS cells were from Novagen (Madison, WI, USA). 1,2-Diheptanoyl-*sn*-glycero-3-phosphocholine (DHPC) and all additional phospholipids used in this study were from Avanti Polar Lipids (Alabaster, AL, USA). N-lauroylsarcosine, sodium cholate, CHAPSO, dimethylformamide (DMF), dithiothreitol (DTT), globulin-free bovine serum albumin (BSA), MES and citrate buffers were from Sigma-Aldrich (St-Louis, MO, USA) whereas carbonate buffer and Triton X-100 were from Fisher Scientific (Montreal, Canada). Octyl β-D-glucopyranoside and n-dodecyl-beta-D-maltoside were from Calbiochem (San Diego, USA). Sodium dodecyl sulfate (SDS), hexane, methanol, ethyl acetate and Tris–HCl were from Laboratoire MAT (Quebec, Canada). Econo-Pac® 10DG and His-Trap columns were respectively from Bio-Rad (Hercules, CA, USA) and GE Healthcare (Piscataway, NJ, USA). All experiments were performed at least in triplicate with different enzyme preparations and the average value was used for the analysis of the data.

2.2. Cloning, expression and purification of tLRAT

tLRAT cDNA was cloned into the pET11a vector, overexpressed in *E. coli* Bl21(DE3) pLysS and purified using His-Trap columns as previously described [31]. In order to perform enzymatic assays in different experimental conditions, the elution buffer was changed to citrate (10 mM, pH 6, 0.05% SDS), MES (10 mM, pH 6, 0.05% SDS) phosphate (10 mM, pH 7.4, 0.05% SDS), Tris–HCl (10 mM, pH 8, 0.05% SDS) or carbonate (10 mM, pH 9.2, 0.05% SDS) buffers using an Econo-Pac® 10DG column.

2.3. Enzymatic assays of tLRAT

A reliable method was conceived to determine the enzyme activity of LRAT in order to characterize its biochemical properties and thermal stability in details. Activity assays have been reported with purified tLRAT produced in *E. coli* [9,14,23,25,27]. However, these experiments performed using water-insoluble substrates (phospholipid and all-*trans* retinol) resulted in values of maximum tLRAT activity which varied significantly from 3.4 [25] to 16.4 [9] and 42 [27] mmol of retinyl ester/min per mol of tLRAT and were much lower than that of LCAT (30,860 mmol of retinyl ester/min per mol of enzyme) (see Table 1 and Section 3.3). Therefore, a protocol has been devised to optimize enzymatic activity of tLRAT using a water-soluble phospholipid (DHPC) acting both as a substrate and as a detergent to solubilize the retinol substrate. The activity of tLRAT was then determined by monitoring the formation of all-trans retinyl heptanoate from all-trans retinol and DHPC. A stock solution of all-*trans* retinol was prepared in DMF. Then, 2.5 μL from this solution was added to a reaction mixture containing 1.25×10^{-2} μg tLRAT, 1% BSA, 6.25 mM DHPC and 1 mM DTT in a total volume of 250 μL to achieve a final concentration of 500 μM retinol. These particular concentrations are very important to obtain a maximum tLRAT activity. Indeed, after many trials and errors, the DHPC:retinol molar ratio was found to be very critical. It should be equal to at least 12.5:1 to allow proper solubilization of retinol by DHPC. In addition, a DHPC:tLRAT molar ratio of 4.2×10^6:1 should not be exceeded, otherwise a large decrease in tLRAT activity occurs. Unless otherwise stated, the tLRAT enzymatic reaction was measured at 20 °C under dim red light using dark Eppendorf tubes under stirring at 400 rpm using the Thermomixer R (Eppendorf). The reaction was then quenched after 15 min by mixing 100 μL of the reaction mixture with 200 μL methanol. The retinoids were extracted by adding 300 μL hexane to the latter mixture and vortexing vigorously for 30 s. Then, 50 μL of this retinoid extract was analyzed by HPLC (Hewlett-Packard 1100 series or a Shimadzu Prominence Modular) equipped with a diode array detector

Table 1
Comparison between the enzymatic properties of tLRAT and tLCAT reported in different studies.

Enzyme	V_{max} (mol of retinyl ester or cholesteryl ester/min per mol of enzyme)	Km (μM)	Catalytic efficiency (M^{-1} s^{-1})	Kcat (s^{-1})
tLRAT[a]	2426 ± 216	55 ± 16	7.3×10^5	40.4
tLRAT[b]	0.0034	0.24	235	5.6×10^{-5}
tLRAT[c]	0.0164	1.67	164	2.7×10^{-4}
tLRAT[d]	0.042	N.A.	N.A.	7×10^{-4}
tLCAT[e]	3.6	3.4	1.76×10^4	0.06
tLCAT[f]	30.86	2.3	2.57×10^5	0.514

[a] Present study.
[b] Bok et al. [25].
[c] Jahng et al. [9].
[d] Xue et al. [27].
[e] Adimoolam et al. [39].
[f] Chisholm et al. [28].

and a Phenomenex Luna Silica analytical normal-phase column (5 μm, 250 mm × 4.6 mm), using hexane: ethyl acetate (90:10) as the eluant at a flow rate of 2 mL/min. The separation of the retinoids by HPLC is shown in the inset of Fig. 1A (see Section 3.2). The retinyl heptanoate absorbance integration peak was converted into moles of product using its molar extinction coefficient of 52,275 M^{-1} cm^{-1} [32,33].

2.4. Assay of chain length specificity of tLRAT

In order to determine the chain length specificity of tLRAT, its activity was measured using a mixture of DHPC (C7:0), used here as detergent to solubilize retinol and the following individual phospholipids with increasing fatty acyl chain length: dioctanoyl (C8:0)-, didecanoyl (C10:0)-, dilauroyl (C12:0)-, dimyristoyl (C14:0)-, dipalmitoyl (C16:0)- and dioleoyl (C18:1)-*sn*-glycero-3-phosphocholine at a molar ratio of 10:1 (DHPC:other phospholipids). After solubilization of these phospholipids in the reaction medium containing DHPC, tLRAT and retinol were added and the activity was determined by comparing the peak of retinyl ester formed (C8:0, C10:0, C12:0, C14:0, C16:0, C18:1) with that of retinyl heptanoate (C7:0).

2.5. pH-, time- and temperature-dependent stability of tLRAT activity

Optimum pH has been determined by measuring tLRAT activity at different pHs using various buffers ranging from pH 4 to 11. The time-dependent enzyme stability has then been determined by measuring the residual activity of tLRAT incubated in different buffers (from pH 6 to 9.2) at a concentration of 1.8 mg/mL for different periods of time, up to 14 days, at 20 °C. Optimal temperature for the tLRAT activity was determined by carrying out the enzymatic assays at different temperatures (10–35 °C). Thermostability was determined by incubating the enzyme at temperatures ranging from 20 to 100 °C. Subsequently, the residual activity was measured at 20 °C as described in Section 2.3. To determine the half-life of tLRAT activity at 100 °C, aliquots of the protein were withdrawn at different periods of time.

2.6. Determination of the secondary structure of tLRAT by circular dichroism and infrared spectroscopy

Circular dichroism measurements were performed using a Jasco spectropolarimeter (Model J-815, Jasco, Easton, MD). These experiments were performed at different temperatures ranging from 20 to 100 °C in citrate buffer using a thin quartz cell with an optical path length of 0.1 cm. The protein concentration has been adjusted to 0.2 mg/ml. For each spectrum, 10 scans were collected from 190 to 260 nm. The buffer contribution was subtracted and the molar ellipcity at ~208 nm was determined. Infrared measurements were made using a Magna 760 FTIR spectrometer from Nicolet (Thermo Scientific, Madison, WI) equipped with a nitrogen-cooled MCT detector. The spectra of tLRAT were measured at different temperatures ranging from 20 to 85 °C. Temperature was adjusted using a home built temperature regulator. The protein samples were incubated at each temperature for 20 min prior to measuring an infrared spectrum. Approximately 30 μL of tLRAT at a concentration of 20 mg/ml in a D_2O buffer containing 10 mM citrate (pH 6) and 0.05% SDS was deposited between the two CaF_2 windows of the Biocell™ (Biotools Inc., Jupiter, FL) manufactured with a calibrated path length of 50 μm. The Biocell™ was placed in a homemade heating system using a Peltier element as a heating/cooling device. To prevent solvent evaporation during the course of long-term heating measurements, outer sealing of the cell was achieved by lubricating with paraffin. Spectra resulted from the acquisition of 128 scans at a resolution of 4 cm^{-1}. The spectral region between 1700 and 1515 cm^{-1} corresponding to the amide region was baseline-corrected using a spline function. All spectra were treated using the Omnic software. The spectrum of buffer was subtracted from all spectra.

3. Results

3.1. Effect of different detergents on tLRAT extraction and enzymatic activity

Detergents are necessary to extract tLRAT from membrane lysates of bacterial cells. Several types of detergents were assayed to find out which one is most appropriate. In contrast to previous data [25], non-ionic detergents such as 0.2% Triton X-100 (cmc = 0.016%), 0.7% CHAPSO (cmc = 0.5%), and 1.2 mM n-dodecyl-beta-D-maltoside (cmc = 0.17 mM) were assayed to extract tLRAT without much success whereas the ionic detergent sodium cholate at a concentration of 28 mM (cmc = 14 mM) was not effective at all. Only two anionic detergents allowed the efficient extraction of tLRAT from the *E. coli* centrifuged lysate pellets: 0.05% SDS (cmc = 0.17–0.23%) and 0.25% N-lauroylsarcosine (cmc = 0.43%). However, only a low level of tLRAT activity was obtained in the presence of N-lauroylsarcosine compared to that in 0.05% SDS. tLRAT is unlikely to be found in cell lysates as inclusion bodies since a concentration of 1.5% N-lauroylsarcosine is necessary to extract proteins from such cell structures [34]. Nevertheless, one could postulate that SDS was only necessary for tLRAT extraction from cell lysates and that it can be removed safely after or during its purification with no detrimental effect on its activity. However, the exchange of SDS during purification for milder detergents such as octyl glucoside or Triton X-100 led to a complete loss of tLRAT activity.

The effect of SDS on tLRAT activity was also investigated. Results showed that the tLRAT enzymatic activity drastically diminished at SDS concentrations below 0.05% and remained unchanged when SDS concentration was increased from 0.05 to 1%. Finally, SDS is very important for tLRAT stability. Indeed, its enzyme activity completely vanished within 24 h when this detergent was removed.

3.2. Determination of the optimal levels of DHPC for tLRAT activity

In order to determine the maximum acyl transferase activity of tLRAT and to thoroughly characterize its biochemical properties, the formation of the ester product (retinyl heptanoate) has been successfully separated from its substrate (retinol) by HPLC (Fig. 1A, inset). It was rather tricky to determine the saturating, optimal levels of DHPC and retinol mainly because DHPC is used both as a substrate and as a detergent to solubilize retinol. Consequently, in order to achieve maximum activity of tLRAT using saturating concentrations of retinol, sufficiently high DHPC concentrations are also needed to properly solubilize retinol and to provide enough heptanoic acid for the ester formation. However, high levels of DHPC inhibit tLRAT activity such that a large number of assays have been performed to find the most appropriate conditions. This is well demonstrated in Fig. 1A which presents the maximum velocity of tLRAT as a function of DHPC concentration. This plot shows that tLRAT reaches its maximum activity at approximately 10 mM DHPC and then decreases. The concentration of DHPC for all experiments was then set to 6.25 mM to avoid any inhibition by this substrate. It is noteworthy that this value is also much larger than the cmc of DHPC (1.4 mM).

In order to further compare the kinetics behavior of tLRAT against monomeric or micellar aggregated forms of the DHPC substrate, its activity was measured at different concentrations of DHPC but at a constant DHPC/retinol ratio of 12.5:1 (see Section 2.3) to make sure that retinol remains highly soluble and thus fully available to the tLRAT molecules (Fig. 1B). It can be seen that the shape of this curve, presenting the variation of the maximum velocity of tLRAT as a function of DHPC concentration, is sigmoidal. It can be observed that the activity of tLRAT continuously increases with the rise in DHPC concentration and reaches its maximal value in the presence of micellar aggregates of this lipid (10 mM) much above its cmc of 1.4 mM (vertical line, Fig. 1B). The concentration of DHPC corresponding to half-maximal activity of tLRAT is approximately 2.4 mM, which is significantly larger

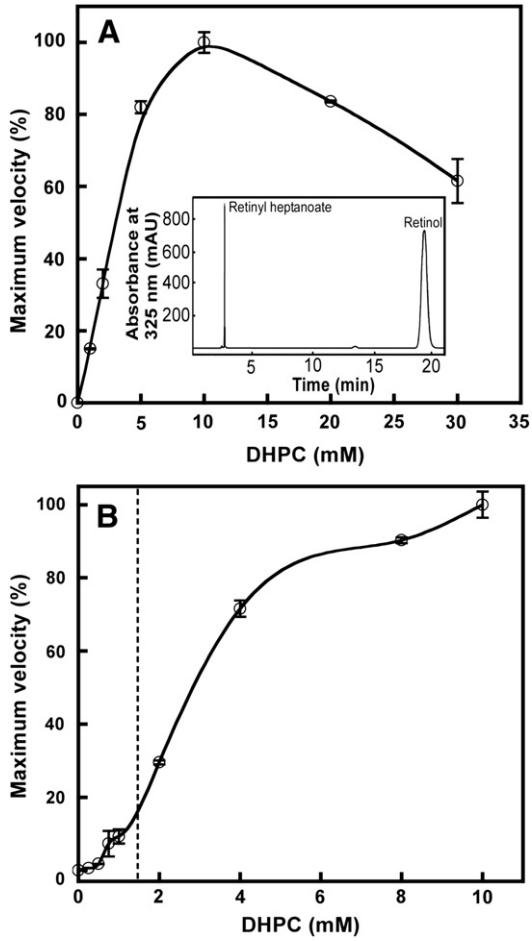

Fig. 1. A: Maximum velocity of tLRAT as a function of DHPC concentration. The velocity was measured in optimal conditions using different concentrations of DHPC, 2.4×10^{-9} mM tLRAT and 500 μM retinol. The experiments were carried out using 1% BSA, 1 mM DTT in a total volume of 250 μL. The tLRAT enzymatic reaction was measured at 20 °C and pH 9.2 under dim red light using dark Eppendorf tubes under stirring at 400 rpm. The reaction was quenched after 15 min. Inset: Typical HPLC chromatogram showing the separation of the retinyl heptanoate extracted from the enzymatic reaction mixture. Retinyl heptanoate and retinol are respectively eluted at ~2.6 and ~19.2 min. B: Hydrolysis of DHPC by tLRAT at a constant DHPC:retinol ratio. Effect of the DHPC concentration on the rate of hydrolysis by tLRAT. Instead of measuring the activity at a constant retinol concentration of 500 μM, the activity presented in this figure was measured at a constant DHPC: retinol ratio of 12.5:1 to make sure that the retinol is fully solubilized by DHPC. Other conditions are the same as in (A). The dotted line indicates the cmc of DHPC (1.4 mM).

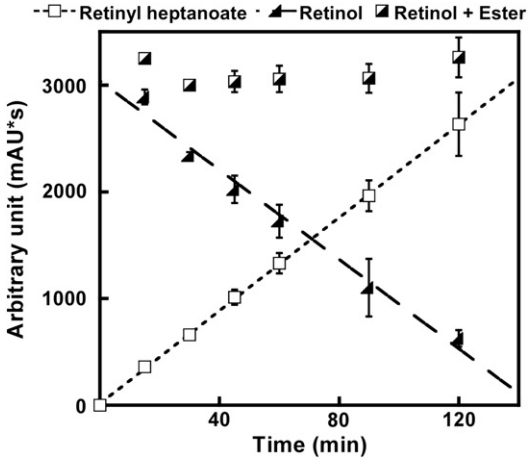

Fig. 2. Kinetic synthesis of retinyl heptanoate and of consumption of retinol by tLRAT. Activity was followed at pH 9.2 and at 20 °C under optimal conditions using 2.4×10^{-9} mM tLRAT, 6.25 mM DHPC and 500 μM retinol. The arbitrary units (mAU*s) presented were determined from the area of the peaks corresponding to the retinyl heptanoate formed or the retinol extracted from the enzymatic reaction mixture at different periods of time.

than the cmc of this lipid. It has been shown that phospholipases are activated by substrate micellar aggregates when their half-maximal enzyme activity was observed at a substrate concentration larger than its cmc [35]. Therefore, these data suggest that tLRAT is showing an *interfacial activation* property such as phospholipases.

3.3. Kinetics behavior of tLRAT with the DHPC and retinol substrates

To study the behavior of tLRAT during the esterification reaction, the kinetics of retinyl heptanoate synthesis and of retinol consumption has been followed under optimal conditions of temperature and pH (see Section 3.5). As shown in Fig. 2, tLRAT exhibited esterification kinetics that remained linear for at least 120 min. tLRAT is thus not inhibited by the presence of retinyl heptanoate which is accumulated in the reaction medium during this period of time. This result is different from that obtained by Berman et al. [36] who showed that the kinetics of esterification by LRAT was only linear for the first 15 min. This behavior might result from an irreversible surface denaturation of LRAT at the lipid–water interface. It has been previously established with lipolytic enzymes [37,38] that such a surface denaturation can be prevented by adding BSA to the reaction mixture. Indeed, the addition of BSA was shown to result in linear kinetic recordings and to prevent lipolytic enzymes from undergoing interfacial denaturation [38]. Kinetic measurements were therefore assayed in the presence and absence of 1% BSA to find out its effect on retinyl ester formation (data not shown). As a result, the addition of BSA to the enzymatic mixture doubled the maximum tLRAT activity. It can thus be concluded that BSA is a useful component in the assay of retinol esterification even in the presence of DHPC, which efficiently solubilizes retinol. Fig. 2 also shows the kinetics of disappearance of retinol during the esterification reaction catalyzed by tLRAT. The consumption of retinol by tLRAT is linear such as that for the synthesis of retinyl heptanoate (Fig. 2). It can also be seen that retinol is still present after 120 min of reaction time.

tLRAT activity was then studied in the presence of different concentrations of retinol. Fig. 3 shows the nonlinear steady state kinetics of tLRAT activity using the Michaelis–Menten equation. It can be seen that tLRAT reaches its maximum activity at approximately 500 μM retinol. Although this concentration exceeds the maximum concentration

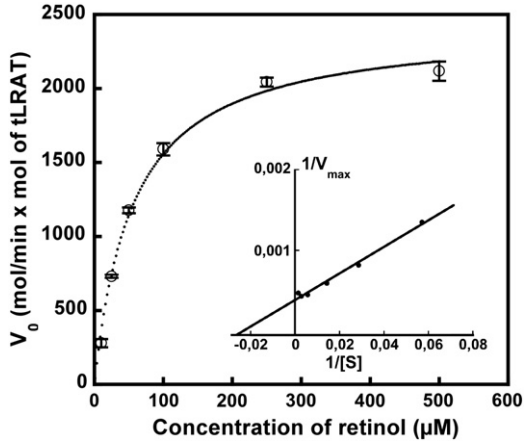

Fig. 3. Non-linear regression analysis of the steady state kinetics of tLRAT using a single rectangular hyperbole function based on the Michaelis–Menten equation. The activity (mol of retinyl ester/min per mol of tLRAT) was measured at optimal conditions using different concentrations of retinol, 2.4×10^{-9} mM tLRAT, 6.25 mM of DHPC. Other conditions are the same as those described in the legend to Fig. 1. Inset: The steady state kinetic study presented in Fig. 3 was graphically represented using a Lineweaver–Burk plot.

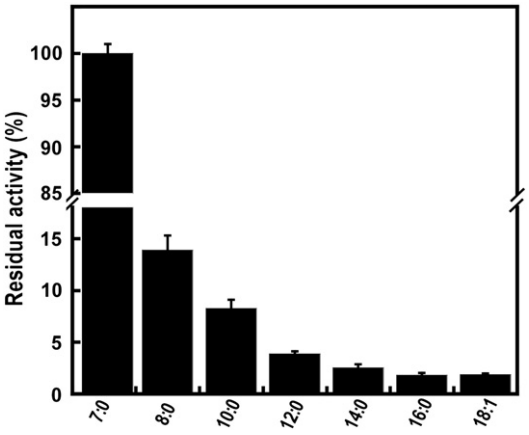

Fig. 4. Substrate specificity of tLRAT. The activity of tLRAT was measured under optimal conditions (see legend to Figs. 1 and 3) using a mixture of DHPC (7:0) with either dioctanoyl (8:0), didecanoyl (10:0), dilauroyl (12:0), dimyristoyl (14:0), dipalmitoyl (16:0) or dioleoyl (18:1) phosphatidylcholines at a molar ratio of 10:1. The residual activity was determined by comparing the peak area of retinyl heptanoate in the HPLC chromatogram to those obtained with the other phopspholipids. 100% activity corresponds to a maximum velocity of 2426 mol of retinyl heptanoate/min per mol of tLRAT.

of retinol reported in tissues or blood, it allowed the performance of an *in vitro* steady state kinetic study of tLRAT (Fig. 3), which was graphically represented using a Lineweaver–Burk plot (see inset of Fig. 3). The parameters of tLRAT esterification activity can be obtained from this plot. Values of V_{max} and Km of respectively 2426 ± 216 mol of retinyl ester/min per mol of tLRAT and of 55 ± 16 μM were precisely determined from a rectangular hyperbole function using a non-linear regression analysis based on the Michaelis–Menten equation (Fig. 3 and Table 1).

3.4. Chain length selectivity of tLRAT

The activity of tLRAT was studied using phospholipids with varying chain lengths in order to determine its dependence on the length of the *sn*-1 fatty acyl moiety of phospholipids. It can be seen in Fig. 4 that tLRAT activity strongly depends on the chain length of the phospholipid substrate. Indeed, tLRAT is highly active towards the short-chain DHPC (C7:0) phospholipid but its enzymatic activity very quickly decreases when phospholipids with longer fatty acyl chains were used as substrates. This result partly agrees with that reported by Golczak and Palczewski [14] who argued that GST-tLRAT acylation at Cys161 was most efficiently catalyzed in the presence of phospholipids containing short fatty acyl chains (C6:0, C7:0, C8:0 and C9:0) on the basis of tLRAT self-acylation by mass spectrometry and of retinyl ester formation by HPLC analyses. In our experiments, a more drastic decrease in tLRAT activity is observed by measuring retinyl ester formation by HPLC (Fig. 4). Indeed, the same retinyl ester absorbance was reported for C6:0 to C9:0 fatty acyl chains [14] whereas, in our experiments (Fig. 4), tLRAT activity in the presence of phospholipids containing C8:0 fatty acyl chains is less than 15% of that observed in the presence of the slightly shorter DHPC (C7:0). Golczak and Palczewski [14] observed no thioester formation by mass spectrometry when using phospholipids with C12:0 fatty acyl chains but a significant formation of C12:0-retinyl esters by HPLC. In our experiments, tLRAT can rather efficiently hydrolyze C12:0 phospholipids (Fig. 4). Indeed, the formation of C12:0-retinyl esters corresponds to approximately 4% of that obtained for C7:0-retinyl esters (Fig. 4), which nonetheless corresponds to a velocity of 92 ± 0.2 mol of retinyl ester/min per mol of tLRAT. This value is ~2000 times larger than the largest tLRAT activity previously reported (Table 1) [27]. Golczak and Palczewski [14] could observe neither protein acylation (thioester formation) with C16:0 fatty acyl chains by mass spectrometry nor the production of C16:0-retinyl esters by HPLC [14]. In contrast, Fig. 4 is showing that tLRAT is able, although less efficiently, to hydrolyze phospholipids with long fatty acyl chains. Indeed, an activity of approximately 46 ± 0.5 mol of retinyl ester/min per mol of tLRAT was obtained when using either the dipalmitoyl(16:0)- or dioleoyl(18:1)-*sn*-glycero-3-phosphocholine substrates (Fig. 4). This value is 1000 times greater than the largest activity previously reported for tLRAT (Table 1) [27]. Therefore, although this activity assay was optimized for water-soluble phospholipids, it should be stressed that phospholipids with short fatty acyl chains, such as DHPC, do not exist in vivo. However, as shown in Fig. 4, the present activity assay can also be used to gain information on tLRAT activity towards phospholipid substrates which are not water-soluble.

3.5. pH and temperature dependence of the enzymatic assay of tLRAT activity

Fig. 5A shows that tLRAT maximum activity is reached at a pH of approximately 9.2 which is consistent with previously reported studies [15,27,40]. However, in contrast to these reports, tLRAT is still active at alkaline pH. Indeed, it presents an activity of approximately 80 and 40% at pH 10 and 10.5, respectively, compared to that at pH 9.2. Fig. 5B shows the variation of maximum tLRAT activity as a function of temperature. It can be seen that the optimal temperature for tLRAT activity is located between 20 and 25 °C. However, tLRAT activity rapidly decreases down to 15% of its initial activity at 35 C.

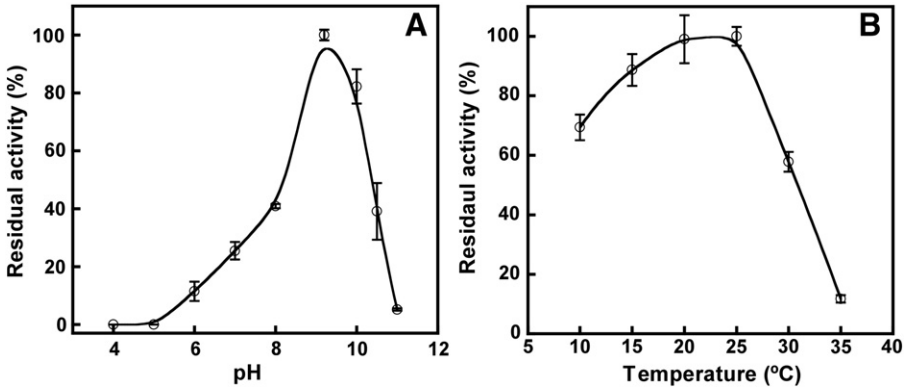

Fig. 5. A: pH-dependent residual activity of tLRAT. The buffers used were citrate (pH 4–6), phosphate (pH 7.4), Tris HCl (pH 8), carbonate (9–10.5) and CAPS (pH 11). The relative activity has been normalized to the highest tLRAT activity at pH 9.2. B: Temperature dependent relative residual activity of tLRAT. The relative activity has been normalized to the highest activity at 20 °C (2 426 mol of retinyl heptanoate/min per mol of tLRAT).

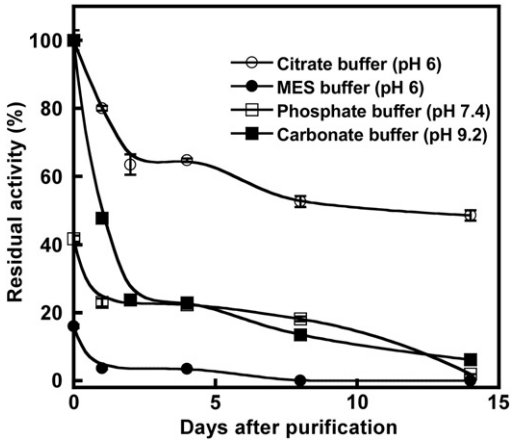

Fig. 6. Residual tLRAT activity as a function of time after purification in different storage buffers: citrate (pH 6), MES (pH 6), phosphate (pH 7.4) and carbonate (pH 9.2). All of these buffers also contain 0.1% SDS. pH- and time-dependent enzyme stability was determined by incubating tLRAT in these buffers at a concentration of 1.8 mg/mL at 20 °C. 100% activity corresponds to the maximum velocity of tLRAT (2 426 mol of retinyl heptanoate/min per mol of enzyme).

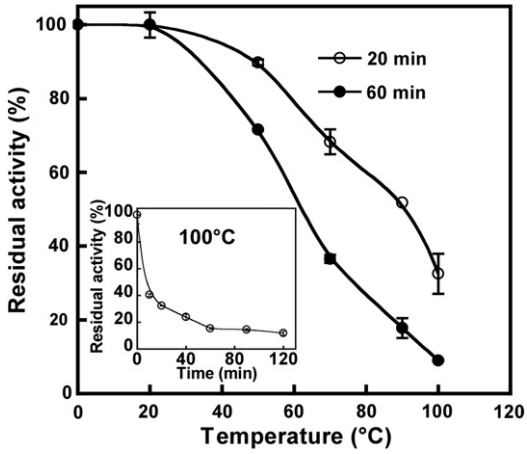

Fig. 7. Stability of tLRAT activity at different temperatures ranging from 20 to 100 °C. tLRAT was pre-incubated at different temperatures for 20 or 60 min. Inset: For temperature stability, the enzyme was pre-incubated at 100 °C for different incubation times from 0 to 120 min. The residual activity was measured at 20 °C. 100% activity corresponds to the maximum velocity of tLRAT (2426 mol of retinyl heptanoate/min per mol of enzyme).

3.6. Dependence of the stability of tLRAT activity on buffer, time and storage temperature

Measurements in different buffers as a function of time were also performed to determine the dependence of the stability of tLRAT activity on these parameters. The data are showing that approximately 52% tLRAT activity is lost 24 h after purification when stored in 10 mM carbonate buffer at pH 9.2 (Fig. 6). In contrast, 80% tLRAT activity is maintained after its incubation for 24 h in 10 mM citrate buffer at pH 6. Moreover, a decrease in enzyme activity of approximately 60 and 84% have respectively been readily observed in phosphate (pH 7.4) and MES buffers (pH 6) after tLRAT purification (Fig. 6). Given that the citrate and MES buffers are at the same pH, these results suggest that the type of buffer is more important than the pH (pH 6) to maintain a stable activity of tLRAT. Moreover, tLRAT was frozen in citrate buffer and stored at −20 and −80 °C or lyophilized and stored at −20 °C for two months. Kinetic studies of these samples showed that tLRAT recovered approximately 90% of its initial activity when thawed from −20 and −80 °C whereas approximately 80% of its activity was retrieved with the lyophilized powder.

3.7. Analysis of the thermal stability of tLRAT

The thermal stability of tLRAT was first determined by measuring its residual activity after incubation of the pure enzyme at temperatures ranging from 20 to 100 °C (Fig. 7). It can be seen that tLRAT is a rather thermostable enzyme as it retained approximately 90, 68, 52 and 33% of its initial activity after 20 min incubation at 50, 70, 90 and 100 °C, respectively. Fig. 7 is also showing that a larger extent of tLRAT activity is lost after 60 min of incubation at the same temperatures. It is however noteworthy that 18 and 9% residual activity is still observed after 60 min of incubation at 90 and 100 °C, respectively. The half-life of tLRAT at 100 °C is 8 min (Fig. 7, inset). Loss of enzyme activity at high temperature is generally accompanied by protein denaturation and a consequent modification of its native structure. Circular dichroism and infrared spectroscopy have thus been used to gather information on temperature dependent structural modifications of tLRAT. Fig. 8 shows circular dichroism spectra of tLRAT at different temperatures. The spectrum at 20 °C is showing two negative bands located at approximately 208 and 222 nm which is typical of a large protein α-helical content. This result is in good agreement with our previous data at this temperature [31]. Moreover, the spectrum at 50 °C is very similar to that at 20 °C. However, an increase in temperature up to 70 °C for 10 (Fig. 8A) or 20 min (Fig. 8B) resulted in a slight decrease in the intensity at 208 nm whereas no change in the signal at 220 nm was observed. The large decrease in molar ellipcity at 208 and 220 nm at 90 and 100 °C strongly suggests that a significant change in the secondary structure of tLRAT takes place at these temperatures (Fig. 8A and B). A plot of the circular dichroism peak intensity at 208 nm as a function of temperature is presented in Fig. 8C. These data are showing that the secondary structure of tLRAT remains stable up to 50 °C during 10 or 20 min. The appearance of tLRAT unfolding can be observed at a temperature of 70 °C. This result is in good agreement with that presented in Fig. 7 showing that tLRAT activity remains almost unchanged up to 50 °C and approximately 68% of its initial activity was retained at 70 °C after 20 min of incubation at this temperature.

Fig. 9A presents the temperature dependence of the amide I′ infrared absorption band of tLRAT. At 20 °C, the maximum of the amide I′ band is located at ~1653 cm^{-1} showing a predominance of α-helices which is consistent with the circular dichroism data (Fig. 8). This band is shifted to larger wavenumbers (~5 cm^{-1}) compared to our previously reported data [31]. This shift can be attributed to a more complete H–D exchange of the peptide bonds because our previous tLRAT sample was lyophilized after solubilization in a D_2O buffer and then dissolved again in D_2O, thus leading to a shift of the amide I′ band toward lower wavenumbers, as previously documented [41]. The width at half height of the amide I′ band is ~59 cm^{-1} which indicates the presence of additional structural components [31]. To obtain more information on the secondary structure of tLRAT, the analysis of the second derivative of the amide I′ band can be performed to identify various secondary structure components in the protein (Fig. 9B). It can be seen that the amide I′ band of tLRAT contains two major bands at 1653 and 1635 cm^{-1} at 20 °C. These components can respectively be attributed to α-helices and β-sheets [31]. No major spectral changes in the amide I′ band are observed between 20 and 50 °C. However, at higher temperatures, it can clearly be seen that the maximum of the amide I′ band progressively shifts to lower wavenumbers together with the appearance of a shoulder (Fig. 9B). From a temperature of 60 °C, the intensity of the band at 1635 cm^{-1} attributed to β-sheet structures is largely reduced with a concomitant appearance of a new band at 1619 cm^{-1}. The spectra at 20 and 85 °C in Fig. 9B have been normalized and compared in Fig. S1. It can be seen that at higher temperatures, the amide I′ becomes broader and not symmetrical. In addition to the disappearance of the band at 1635 cm^{-1} attributed to β-sheets, the new component appearing at 1619 cm^{-1} and the band broadening indicate the presence of non structured components and β-sheet aggregation.

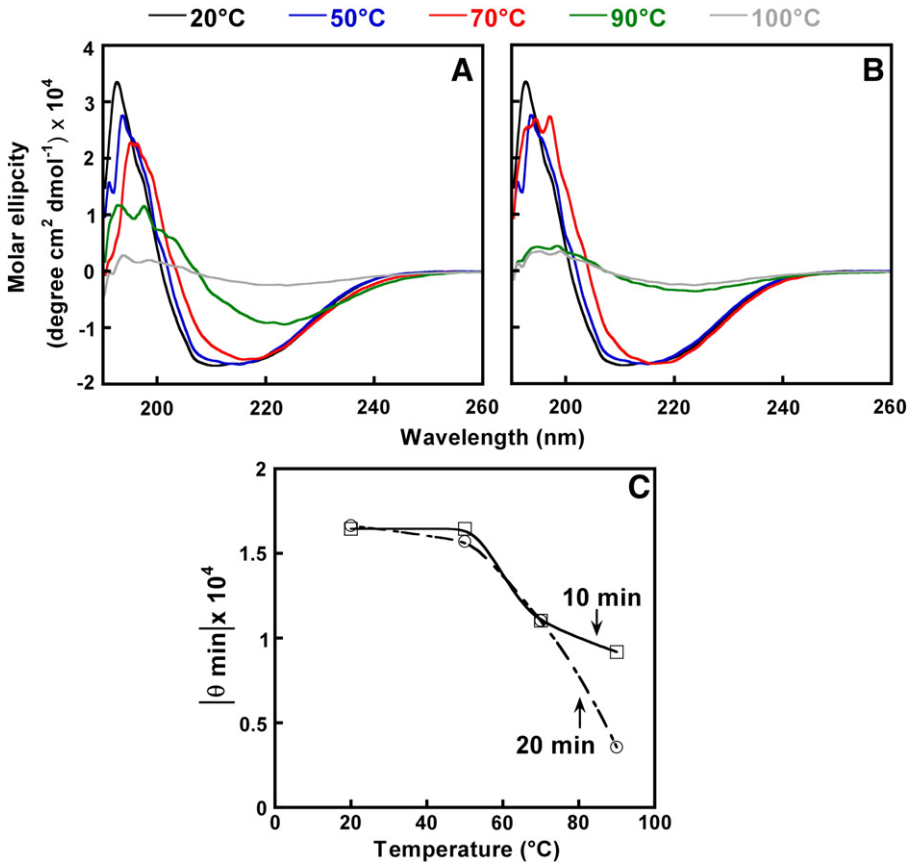

Fig. 8. Circular dichroism spectra of tLRAT as a function of temperature. tLRAT at a concentration of 0.2 mg/ml in citrate buffer was incubated for 10 (A) or 20 min (B) at temperatures ranging from 20 to 100 °C. (C) Plot of the molar ellipcity of tLRAT at ~208 nm after incubation for 10 min or 20 min at different temperatures.

4. Discussion

Previous data have shown that the enzymatic activity of tLRAT is close to 1000 times smaller than that of an enzyme with a comparable activity (LCAT, Table 1). This result was surprising and motivated a thorough characterization of the enzymatic activity and stability of tLRAT using *in vitro* assay conditions. The esterification reaction by tLRAT as a function of DHPC concentration shows a typical Michaelis–Menten dependence of the enzyme activity on substrate concentration (Fig. 3). The decrease of tLRAT activity down to ~60% at 30 mM DHPC can be attributed to a destabilization of the tLRAT structure at this DHPC concentration or to an excessive amount of this substrate compared to the second retinol substrate (the DHPC:retinol ratio increases from 20 to 60 at 10 and 30 mM DHPC, respectively). The data shown in Fig. 1B suggest that tLRAT possesses an *interfacial activation* property such as phospholipases. In contrast, Golczak and Palczewski [14] have shown data suggesting that aggregation of DHPC above its cmc inhibits tLRAT self-acylation. Consequently, they concluded that the lipid–water interface of micellar aggregates is not accessible to tLRAT. In order to properly explain this discrepancy, one should first recall the mechanism of LRAT catalysis. LRAT first hydrolyzes the *sn*-1 fatty acyl chain of phospholipids, which is then used for the self-acylation of its Cys161. LRAT then transfers this fatty acyl chain to retinol to form the retinyl ester product [1,2,4,14]. Golczak and Palczewski [14] and the present study have respectively looked at the effect of DHPC concentration on either the self-acylation of tLRAT in the absence of the retinol substrate or on the esterification of retinol. One can postulate that micellar concentrations of DHPC could inhibit the first step of the catalysis of tLRAT, in the

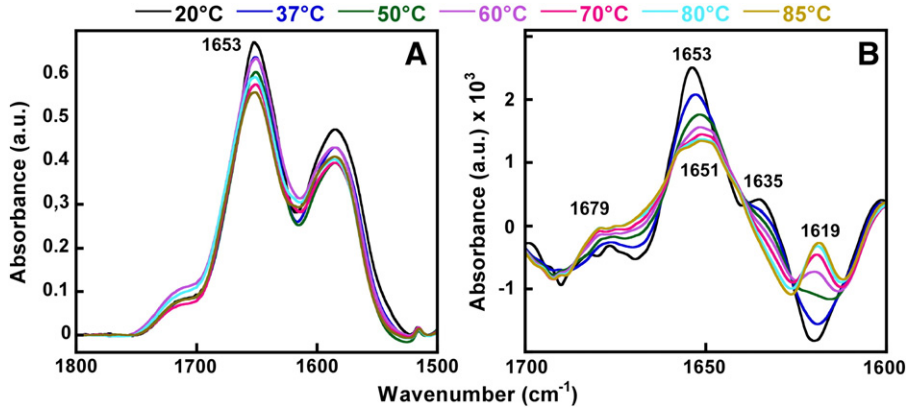

Fig. 9. A: Infrared spectra of tLRAT measured at various temperatures ranging from 20 to 100 °C. The concentration of tLRAT is 20 mg/ml in a D_2O buffer containing 10 mM citrate (pH 6) and 0.05% SDS. B: Second derivative spectra of the amide I′ of tLRAT at different temperatures.

absence of retinol, thus resulting solely in its self-acylation [14], but would enhance the esterification reaction in the presence of the retinol substrate. tLRAT might be unable to further interact with its phospholipid substrate once it reached 50–60% self-acylation in the absence of retinol [14]. Altogether, the present data suggest that the optimal concentration of 6.25 mM DHPC, which is larger than its CMC (1.4 mM), insures a proper solubilization of the retinol substrate and of the other reagents. Therefore, given that DHPC acts both as a detergent and a substrate, tLRAT can have direct access to the phospholipid and retinol substrates, thus promoting its maximal enzymatic activity.

The value of V_{max} of 2426 ± 216 mol of retinyl ester/min per mol of tLRAT reported in the present study is more than 55,000 folds larger than the highest activity reported in the literature for tLRAT (0.042 mol of retinyl ester/min per mol of tLRAT, Table 1 [27]). Moreover, the K_m of 55 ± 16 μM is also much larger than the previously reported values of 0.24 μM [25] and 1.67 μM [9] (Table 1). The discrepancy between these data could be attributed to differences in the experimental conditions between our experiments and those of Bok et al. [25] and Jahng et al. [9]. Indeed, these authors have used a phospholipid substrate (DPPC, 1,2-dipalmitoyl-*sn*-glycero-3-phosphocholine) that is not water soluble even in the presence of CHAPSO because the concentration they used for this detergent (0.1%) was much lower than its cmc (0.5%). In contrast, in our experiments, DHPC is highly water-soluble and it promotes the enzymatic activity of tLRAT by acting both as a detergent and a substrate, as well as by solubilizing the retinol substrate. This discrepancy could also be explained by a better purity of our tLRAT samples [31] compared to those of Bok et al. [25] and Jahng et al. [9] or by a larger affinity of tLRAT for short chain phospholipids, such as DHPC, compared to DPPC, such as is shown in Fig. 4. In this regard, it has recently been proposed that tLRAT preferentially transfers short phospholipid fatty acyl chains on retinol whereas full length LRAT (unpurified from bovine RPE extracts) predominantly produces esters of retinol with long fatty acyl chains [14]. However, in these experiments [14], no maximum tLRAT and LRAT activity has been determined for the phospholipids studied and the concentration of their substrates (10 μM retinol and 1 mM phospholipid) was most likely below the saturation level necessary to obtain the maximum activity of an enzyme [42]. Nonetheless, in our experiments, a very large tLRAT activity has been obtained when using either the dipalmitoyl(16:0)- or dioleoyl(18:1)-*sn*-glycero-3-phosphocholine substrates (Fig. 4) compared to previously reported data [9,25,27].

The catalytic efficiency (K_{cat}/K_m) of tLRAT to hydrolyze and transfer phospholipid fatty acyl chains to retinol is approximately 7.3×10^5 M^{-1} s^{-1}, which is much larger than the values reported previously by Bok et al. (235 M^{-1} s^{-1}) [25] and Jahng et al. (164 M^{-1} s^{-1}) [9] (Table 1). This catalytic efficiency of tLRAT is larger than that of urease and chymotrypsin but smaller than that of several other enzymes [42] which, however, bear a single enzymatic activity. Indeed, this catalytic efficiency of 7.3×10^5 M^{-1} s^{-1} includes the two enzymatic activities of LRAT since we have measured the production of retinyl esters. It is thus more appropriate to compare the enzymatic properties of tLRAT with those of an enzyme with a similar activity, i.e. LCAT, which also bears two enzymatic activities, such as those of tLRAT (phospholipase and esterifying activities). The largest catalytic efficiency reported for LCAT is 3 times smaller than the present value [28] (Table 1).

The activity versus temperature curve (Fig. 4B) showed a maximal retinyl ester formation between 20 and 25 °C and the activity drastically diminished at higher temperatures, showing a very low activity level at 35 °C. All previous activity measurements with tLRAT were performed at room temperature [9,25,27,43]. Only Golczak and Palczewski [14] reported an enzymatic activity of purified tLRAT in fusion with GST at 37 °C. It can thus be postulated that GST could provide stability to tLRAT, although no specific activity data were reported by these authors. The much higher activity of tLRAT observed at room temperature compared to that at 35 °C could be explained by the absence of its N- and C-terminal alpha helices. Indeed, in view of the membrane location of the substrates of LRAT, it is conceivable that the presence of its N- and C-terminal alpha helices would allow the anchoring of LRAT to the membrane [24], thereby resulting in a more stable structure and enzyme activity. It would thus be interesting to find out whether a single or both terminal alpha helices are necessary to observe a robust enzymatic activity of LRAT at 37 °C given the recent proposal that only its C-terminal transmembrane domain is essential for membrane targeting [23] and our recent data allowing us to postulate that both N- and C-terminal hydrophobic α-helical peptides behave similarly and could thus both serve to anchor tLRAT to the membrane [24].

Among the different parameters assayed, the storage buffer has a largest effect on tLRAT stability. Using the citrate or MES buffer at the same pH 6, tLRAT presented a very different behavior. Indeed, more than 65% activity was remaining 4 days after purification of tLRAT in citrate buffer at room temperature in contrast to ~3% in the MES buffer in the same conditions. tLRAT thus appears as a highly stable protein at least at this temperature and in this buffer. In comparison, enzymes such as lipases require the use of "room temperature ionic liquids" to provide them stability [44]. This is obviously not necessary in the case of tLRAT.

Another interesting feature of tLRAT is its thermal stability. The study of the effect of different temperatures on the activity and structural properties of tLRAT allowed us to find out that it is a rather stable enzyme. Only high temperatures resulted in a detrimental effect on its enzymatic stability and structure. Indeed, the spectroscopic data showed that tLRAT is quite thermostable and changes in its secondary structure can be observed only at temperatures from 60 °C. tLRAT contains a large proportion of α-helical and β-sheet structural elements [31]. The incubation of tLRAT at high temperatures (>60 °C) progressively turned out in the formation of aggregated β-sheets at the expense of the α-helical and β-sheet structural components.

It is interesting to compare the stability of tlRAT with that of other thermostable proteins. Recently, Potvin-Fournier et al. [41] have demonstrated that bovine recoverin is thermostable up to 65 °C only in the presence of excess of calcium ions. Importantly, tLRAT remains active after its incubation at 100 °C for 20 or 60 min without the addition of stabilizing excipients or preservatives such as glycerol, β-cyclodextrin, salts, and calcium. Clark and colleagues [45] have investigated the spectral changes in the amide I′ region of bovine serum albumin (BSA), lysozyme, insulin, ribonuclease and chymotrypsin at temperatures ranging from 25 to 95 °C. They observed a new band typical of aggregation at ~1620 cm^{-1} at temperatures >60 °C for all of these proteins. Similarly to our observations with tLRAT, the increase in temperature resulted in the appearance of a band at ~1620 cm^{-1} at the expense of the other components. A review on protein aggregation by Dong et al. [46] illustrated the thermally-induced aggregation of several additional proteins from different sources, i.e. azurin [47], cholera toxin [48], adenylate cyclase [49], cytochrome c [50], chymotrypsinogen [51], concanavalin A [52], acetylcholine receptor [53], glucoamylase [54], acetylcholinesterase [55], and transglutaminase [56] which have also been characterized by using the second-derivative of the amide I′ band of their infrared spectra. In all of these studies, a common feature of thermally-induced protein aggregation is the formation of intermolecular aggregated β-sheets [46] at temperatures ranging from 40 to 76 °C. Although signs of aggregation of tLRAT could be observed at 70 °C (Fig. 9B), the enzyme respectively exhibited ~90 and 70% of its initial activity after 20 or 60 min of incubation time at this temperature. tLRAT thus appears to be more thermostable than the above proteins. This behavior could be related to the instability of tLRAT in its "opened" conformation in the presence of its substrates or to the absence of its N- and C-terminal alpha helices.

In conclusion, very high rates of retinyl ester formation by tLRAT were observed with a high reproducibility. The present study allowed us to thoroughly characterize the properties of this enzyme and to determine its time- and temperature-dependent stability as

well as its substrate specificity. It thus allowed us to significantly improve our understanding of the structure–function relationship of this enzyme.

Supplementary data to this article can be found online at http://dx.doi.org/10.1016/j.bbapap.2014.02.022.

Acknowledgements

The work described was supported by the Canadian Institutes of Health Research (CIHR). S. Bussières was a recipient of the Frederick Banting and Charles Best Graduate Scholarship from the CIHR. M. Lhor was awarded a scholarship from the Regroupement Stratégique PROTEO, which is supported by the FRQNT. The Banque d'Yeux Nationale is partly supported by the Réseau de Recherche en Santé de la Vision from the FRQS.

References

[1] P.N. MacDonald, D.E. Ong, Evidence for a lecithin-retinol acyltransferase activity in the rat small intestine, J. Biol. Chem. 263 (1988) 12478–12482.
[2] J.C. Saari, D.L. Bredberg, Lecithin:retinol acyltransferase in retinal pigment epithelial microsomes, J. Biol. Chem. 264 (1989) 8636–8640.
[3] M.C. Schmitt, D.E. Ong, Expression of cellular retinol-binding protein and lecithin-retinol acyltransferase in developing rat testis, Biol. Reprod. 49 (1993) 972–979.
[4] P.N. MacDonald, D.E. Ong, A lecithin:retinol acyltransferase activity in human and rat liver, Biochem. Biophys. Res. Commun. 156 (1988) 157–163.
[5] O.L. Francone, C.J. Fielding, Structure–function relationships in human lecithin:cholesterol acyltransferase. Site-directed mutagenesis at serine residues 181 and 216, Biochemistry 30 (1991) 10074–10077.
[6] O.L. Francone, C.J. Fielding, Effects of site-directed mutagenesis at residues cysteine-31 and cysteine-184 on lecithin–cholesterol acyltransferase activity, Proc. Natl. Acad. Sci. U. S. A. 88 (1991) 1716–1720.
[7] R.R. Rando, The biochemistry of the visual cycle, Chem. Rev. 101 (2001) 1881–1896.
[8] A. Ruiz, A. Winston, Y.-H. Lim, B.A. Gilbert, R.R. Rando, D. Bok, Molecular and biochemical characterization of lecithin retinol acyltransferase, J. Biol. Chem. 274 (1999) 3834–3841.
[9] W.J. Jahng, L. Xue, R.R. Rando, Lecithin retinol acyltransferase is a founder member of a novel family of enzymes, Biochemistry 42 (2003) 12805–12812.
[10] P.J. Hughes, G. Stanway, The 2A proteins of three diverse picornaviruses are related to each other and to the H-rev107 family of proteins involved in the control of cell proliferation, J. Gen. Virol. 81 (2000) 201–207.
[11] A. Hajnal, R. Klemenz, R. Schafer, Subtraction cloning of H-rev107, a gene specifically expressed in H-ras resistant fibroblasts, Oncogene 9 (1994) 479–490.
[12] W. Hanna-Rose, M. Han, The *Caenorhabditis elegans* EGL-26 protein mediates vulval cell morphogenesis, Dev. Biol. 241 (2002) 247–258.
[13] C. Sers, U. Emmenegger, K. Husmann, K. Bucher, A.C. Andres, R. Schafer, Growth-inhibitory activity and downregulation of the class II tumor-suppressor gene H-rev107 in tumor cell lines and experimental tumors, J. Cell Biol. 136 (1997) 935–944.
[14] M. Golczak, K. Palczewski, An acyl-covalent enzyme intermediate of lecithin:retinol acyltransferase, J. Biol. Chem. 285 (2010) 29217–29222.
[15] M.S. Mondal, A. Ruiz, D. Bok, R.R. Rando, Lecithin retinol acyltransferase contains cysteine residues essential for catalysis, Biochemistry 39 (2000) 5215–5220.
[16] M. Jin, S. Li, W.N. Moghrabi, H. Sun, G.H. Travis, Rpe65 is the retinoid isomerase in bovine retinal pigment epithelium, Cell 122 (2005) 449–459.
[17] G. Moiseyev, Y. Chen, Y. Takahashi, B.X. Wu, J.X. Ma, RPE65 is the isomerohydrolase in the retinoid visual cycle, Proc. Natl. Acad. Sci. U. S. A. 102 (2005) 12413–12418.
[18] P.D. Kiser, M. Golczak, A. Maeda, K. Palczewski, Key enzymes of the retinoid (visual) cycle in vertebrate retina, Biochim. Biophys. Acta 1821 (2012) 137–151.
[19] J.C. Saari, Vitamin A metabolism in rod and cone visual cycles, Annu. Rev. Nutr. 32 (2012) 125–145.
[20] T.D. Lamb, E.N. Pugh Jr., Dark adaptation and the retinoid cycle of vision, Prog. Retin. Eye Res. 23 (2004) 307–380.
[21] J. von Lintig, P.D. Kiser, M. Golczak, K. Palczewski, The biochemical and structural basis for trans-to-cis isomerization of retinoids in the chemistry of vision, Trends Biochem. Sci. 35 (2010) 400–410.
[22] R.O. Parker, R.K. Crouch, Retinol dehydrogenases (RDHs) in the visual cycle, Exp. Eye Res. 91 (2010) 788–792.
[23] A.R. Moise, M. Golczak, Y. Imanishi, K. Palczewski, Topology and membrane association of lecithin: retinol acyltransferase, J. Biol. Chem. 282 (2007) 2081–2090.
[24] S. Bussières, L. Cantin, B. Desbat, C. Salesse, Binding of a truncated form of lecithin: retinol acyltransferase and its N- and C-terminal peptides to lipid monolayers, Langmuir 28 (2012) 3516–3523.
[25] D. Bok, A. Ruiz, O. Yaron, W.J. Jahng, A. Ray, L. Xue, R.R. Rando, Purification and characterization of a transmembrane domain-deleted form of lecithin retinol acyltransferase, Biochemistry 42 (2003) 6090–6098.
[26] R.R. Rando, Membrane-bound lecithin-retinol acyltransferase, Biochem. Biophys. Res. Commun. 292 (2002) 1243–1250.
[27] L. Xue, R.R. Rando, Roles of cysteine 161 and tyrosine 154 in the lecithin retinol acyltransferase mechanism, Biochemistry 43 (2004) 6120–6126.
[28] J.W. Chisholm, A.K. Gebre, J.S. Parks, Characterization of C-terminal histidine-tagged human recombinant lecithin:cholesterol acyltransferase, J. Lipid Res. 40 (1999) 1512–1519.
[29] I. Bustos-Jaimes, R. Mora-Lugo, M.L. Calcagno, A. Farrés, Kinetic studies of Gly28:Ser mutant form of Bacillus pumilus lipase: Changes in kcat and thermal dependence, Biochim. Biophys. Acta 1804 (2010) 2222–2227.
[30] N.C. Benson, V. Daggett, Dynameomics: large-scale assessment of native protein flexibility, Protein Sci. 17 (2008) 2038–2050.
[31] S. Bussières, T. Buffeteau, B. Desbat, R. Breton, C. Salesse, Secondary structure of a truncated form of lecithin retinol acyltransferase in solution and evidence for its binding and hydrolytic action in monolayers, Biochim. Biophys. Acta 1778 (2008) 1324–1334.
[32] J. Boldnigh, H.R. Camma, F.D. Collins, R.A. Morton, N.T. Gridgeman, O. Isler, M. Kofler, R.J. Taylor, A.S. Welland, T. Bradbury, Pure all-trans vitamin A acetate and the assessment of vitamin A potency by spectrophotometry, Nature (London) 168 (1951) 598.
[33] A.C. Ross, Separation and quantitation of retinyl esters and retinol by high-performance liquid chromatography, Methods Enzymol. 123 (1986) 68–74.
[34] E. Trudel, S. Beaufils, A. Renault, R. Breton, C. Salesse, Binding of RPE65 fragments to lipid monolayers and identification of its partners by glutathione S-transferase pull-down assays, Biochemistry 45 (2006) 3337–3347.
[35] R. Verger, G.H. De Haas, Interfacial enzyme kinetics of lipolysis, Annu. Rev. Biophys. Bioeng. 5 (1976) 77–117.
[36] E.R. Berman, J. Horowitz, N. Segal, S. Fisher, L. Feeney-Burns, Enzymatic esterification of vitamin A in the pigment epithelium of bovine retina, Biochim. Biophys. Acta 630 (1980) 36–46.
[37] Y. Gargouri, G. Pieroni, P.A. Lowe, L. Sarda, R. Verger, Human gastric lipase, Eur. J. Biochem. 156 (1986) 305–310.
[38] Y. Ben Ali, H. Chahinian, S. Petry, G. Muller, F. Carrière, R. Verger, A. Abousalham, Might the kinetic behavior of hormone-sensitive lipase reflect the absence of the lid domain? Biochemistry 43 (2004) 9298–9306.
[39] S. Adimoolam, L. Jin, E. Grabbe, J.J. Shieh, A. Jonas, Structural and functional properties of two mutants of lecithin-cholesterol acyltransferase (T123I and N228K), J. Biol. Chem. 273 (1998) 32561–32567.
[40] S. Furuyoshi, Y.Q. Shi, R.R. Rando, Acyl group transfer from the sn-1 position of phospholipids in the biosynthesis of n-dodecyl palmitate, Biochemistry 32 (1993) 5425–5430.
[41] K. Potvin-Fournier, T. Lefèvre, A. Picard-Lafond, G. Valois-Paillard, L. Cantin, C. Salesse, M. Auger, The thermal stability of recoverin depends on calcium binding and its myristoyl moiety as revealed by infrared spectroscopy, Biochemistry 53 (2013) 48–56.
[42] V. Voet, J.G. Voet, Biochemistry, John Wiley & Sons, 1997.
[43] L. Xue, W.J. Jahng, D. Gollapalli, R.R. Rando, Palmitoyl transferase activity of lecithin retinol acyl transferase, Biochemistry 45 (2006) 10710–10718.
[44] J.L. Kaar, Lipase activation and stabilization in room-temperature ionic liquids, Methods Mol. Biol. 679 (2011) 25–35.
[45] A. Clark, D. Saunderson, A. Suggett, Infrared and laser-Raman spectroscopic studies of thermally-induced globular protein gels, Int. J. Pept. Protein Res. 17 (1981) 353–364.
[46] A. Dong, S. Prestrelski, S. Allison, J. Carpenter, Infrared spectroscopic studies of lyophilization- and temperature-induced protein aggregation, J. Pharm. Sci. 84 (1995) 415–424.
[47] W.K. Surewicz, A.G. Szabo, H.H. Mantsch, Conformational properties of azurin in solution as determined from resolution-enhanced Fourier-transform infrared spectra, Eur. J. Biochem. 167 (1987) 519–523.
[48] W. Surewicz, J. Leddy, H. Mantsch, Structure, stability, and receptor interaction of cholera toxin as studied by Fourier-transform infrared spectroscopy, Biochemistry 29 (1990) 8106–8111.
[49] E. Labruyere, M. Mock, W.K. Surewicz, H.H. Mantsch, T. Rose, H. Munier, R.S. Sarfati, O. Barzu, Structural and ligand-binding properties of a truncated form of *Bacillus anthracis* adenylate cyclase and of a catalytically inactive variant in which glutamine substitutes for lysine-346, Biochemistry 30 (1991) 2619–2624.
[50] A. Muga, H.H. Mantsch, W.K. Surewicz, Membrane binding induces destabilization of cytochrome c structure, Biochemistry 30 (1991) 7219–7224.
[51] A.A. Ismail, H.H. Mantsch, P.T.T. Wong, Aggregation of chymotrypsinogen: portrait by infrared spectroscopy, Biochim. Biophys. Acta 1121 (1992) 183–188.
[52] M. Jackson, H.H. Mantsch, The use and misuse of FTIR spectroscopy in the determination of protein structure, Crit. Rev. Biochem. Mol. Biol. 30 (1995) 95–120.
[53] T. Theophanides, J. Anastassopoulou, N. Fotopoulos, U. Görne-Tschelnokow, D. Naumann, W. Mäntele, C. Schultz, F. Hucho, FTIR studies of the acetylcholine receptor; secondary structure, temperature behaviour, agonist induced changes and linear dichroitic measurements, Fifth International Conference on the Spectroscopy of Biological Molecules, 1993, pp. 403–404.
[54] M. Urbanova, P. Pancoska, T.A. Keiderling, Spectroscopic study of the temperature-dependent conformation of glucoamylase, Biochim. Biophys. Acta 1203 (1993) 290–294.
[55] U. Görne-Tschelnokow, D. Naumann, C. Weise, F. Hucho, Secondary structure and temperature behaviour of acetylcholinesterase, Eur. J. Biochem. 213 (1993) 1235–1242.
[56] F. Tanfani, E. Bertoli, M. Signorini, C.M. Bergamini, Structural investigation of transglutaminase by Fourier transform infrared spectroscopy, Eur. J. Biochem. 218 (1993) 499–505